APJAI
Asian Pacific Journal of
Allergy and Immunology

ORIGINAL ARTICLE

Biological properties of reverse ankyrin engineered for dimer construction to enhance HIV-1 capsid interaction

On-anong Juntit,[1,3] Umpa Yasamut,[1,3,4] Supachai Sakkhachornphop,[2] Koollawat Chupradit,[1,3] Weeraya Thongkum,[3,4] Chatchawan Srisawat,[5] Tawan Chokepaichitkool,[6] Prachya Kongtawelert,[6] Chatchai Tayapiwatana[1,3,4]

Abstract

Background: Assembly and budding in the late-stage of human immunodeficiency virus type 1 (HIV-1) production rely on Gag protein polymerization at the inner leaflet of the plasma membrane. We previously generated a monomeric ankyrin repeat protein (Ank1D4) that specifically interacts with capsid protein (CAp24) of HIV-1, however this protein had modest binding affinity.

Objective: This study aimed to improve the avidity of Ank1D4 by generating two Ank1D4 dimers: ($Ank1D4_{NC-NC}$) and its inverted form ($Ank1D4_{NC-CN}$), with each domain connected by a flexible $(G_4S)_4$ linker peptide.

Methods: Binding properties of monomeric and dimeric Ank1D4 was performed by capture enzyme-linked immunosorbent assay (ELISA). Sandwich ELISA was used to examine bifunctional module of dimeric Ank1D4. $Ank1D4_{NC-NC}$ and $Ank1D4_{NC-CN}$ were evaluated using bio-layer interferometry (BLI), compared to monomeric Ank1D4.

Results: Similar binding surfaces were observed in both dimers which was comparable with monomeric Ank1D4. The interaction of $Ank1D4_{NC-CN}$ with CAp24 was significantly greater than that of $Ank1D4_{NC-NC}$ and Ank1D4 by capture ELISA. $Ank1D4_{NC-CN}$ also exhibited bifunctionality using a sandwich ELISA. The KD of $Ank1D4_{NC-CN}$, $Ank1D4_{NC-NC}$ and monomeric Ank1D4 was 3.5 nM, 53.7 nM, and 126.2 nM, respectively using bio-layer interferometry analysis.

Conclusions: This study provides a strategy for increasing Ank1D4 avidity through the construction of novel inverted dimers with a flexible linker. $Ank1D4_{NC-CN}$ may provide an alternative treatment strategy for inhibiting HIV-1 replication.

Key words: Ankyrins, Ankyrin dimer, Binding kinetics, Capsid proteins, HIV-1

Citation:
Juntit, O., Yasamut, U., Sakkhachornphop, S., Chupradit, K., Thongkum, W., Srisawat, C., Chokepaichitkool, T., Kongtawelert, P., Tayapiwatana, C. (2025). Biological properties of reverse ankyrin engineered for dimer construction to enhance HIV-1 capsid interaction. *Asian Pac J Allergy Immunol*, 43(3), 737-744. https://doi.org/10.12932/ap-210122-1310

Affiliations:
[1] Division of Clinical Immunology, Department of Medical Technology, Faculty of Associated Medical Sciences, Chiang Mai University, Chiang Mai, Thailand
[2] Research Institute for Health Sciences, Chiang Mai University, Chiang Mai, Thailand
[3] Center of Biomolecular Therapy and Diagnostic, Faculty of Associated Medical Sciences, Chiang Mai University, Chiang Mai, Thailand
[4] Center of Innovative Immunodiagnostic Development, Department of Medical Technology, Faculty of Associated Medical Sciences, Chiang Mai University, Chiang Mai, Thailand
[5] Department of Biochemistry, Faculty of Medicine Siriraj Hospital, Mahidol University, Bangkok, Thailand
[6] Thailand Excellence Center for Tissue Engineering and Stem Cells, Department of Biochemistry, Faculty of Medicine, Chiang Mai University, Chiang Mai, Thailand

Corresponding author:
Chatchai Tayapiwatana
Division of Clinical Immunology, Department of Medical Technology, Faculty of Associated Medical Sciences, Chiang Mai University
110 Intavaroros road, Suthep, Chiang Mai 50200, Thailand
E-mail: chatchai.t@cmu.ac.th

Introduction

Diverse antibody alternatives using non-immunoglobulin (non-Ig) scaffolds have attracted considerable attention over the last decade because of their compact size, stability, and solubility.[1] They include knottins, Kunitz domains, repebodies, alpha repeat proteins (αRep), and designed ankyrin repeat proteins (DARPins).[2–5] These scaffolds enable specific binding to targets mediating protein-protein interactions. Non-Ig scaffolds are advantageous therapeutic agents because they are rapidly cleared from the bloodstream by renal filtration.[5] Recently, the U.S. Food and Drug Administration (FDA) approved the use of two knottin peptide scaffolds: ziconotide for the treatment of neuropathic pain by targeting N-type voltage-sensitive calcium channels, and linaclotide for the treatment of irritable bowel disease. Meanwhile, neovascular age-related macular degeneration (AMD) was treated with a larger scaffold (abicipar pegol, a DARPin).[5] Other larger scaffolds currently in clinical trials include vascular endothelial growth factor A (VEGF-A) specific MP0112 and human epidermal growth factor receptor 2 (HER2) specific DARPin ankyrin (MP0274). Human DARPin specific to CD4 competes with envelope glycoprotein (gp120) of human immunodeficiency virus 1 (HIV-1) and strongly inhibits HIV entry.[6] We previously showed the specific extracellular targeting of DARPin to capsid domain (CAp24) of HIV-1 Gag protein and proposed that DARPin interferes with late-stage HIV-1 assembly *in vivo*.[7,8] In addition, alpha-helicoidal HEAT-like repeat protein scaffolds (αRep) target HIV-1 Gag polyprotein resulting in impaired viral packaging and Gag processing.[2] DARPins and αRep lack disulfide bonds[2,7] making them suitable cytoplasmic targets in a reducing environment.

HIV remains a global public health concern, with the efficacious antiretroviral drug therapy often causing adverse effects due to prolonged use, which may result in drug resistance.[9,10] The drawbacks of antiretroviral therapy have driven the need for the development of HIV gene therapy. The first successful case of gene therapy tackled HIV-1 resistance in a Berlin patient with a homozygous deletion for chemokine receptor 5 (CCR5).[11] Since CCR5 participates in several cellular mechanisms, other strategies were anticipated. Antibodies MF85 scFV[12] and scFv 183-H12-5C[13] were generated against recombinant p24 of HIV-1 to reduce HIV-1 replication. However, incorrect folding in the reducing environment of the cytoplasm and nucleus leads to the loss of antibody activity. An alternative strategy using DARPins and αRep successfully targeted Gag protein of HIV.

The function of Ank1D4 as a specific CAp24 domain inhibitor of HIV Gag should be improved since it has low binding affinity.[14] Meanwhile, mutation of Ank1D4 to Ank1D4-S45Y partly improved the binding affinity from 109 nM to 45 nM in our previous work.[14] Ank1D4-S45Y significantly inhibited either HIV-1 wild-type or the HIV maturation inhibitor-resistant strain for intracellular activity.[15] In this study, we aimed to construct the dimeric form of Ank1D4 to improve avidity. The construction of a functional homo-dimer requires an appropriate linker sequence with a particular amino acid composition. Bioinformatic algorithms previously developed to select the proper linker sequence such as LINKER[16] and SynLinker[17] are no longer active. Generally, $(GGGGS)_n$ provides tremendous flexibility with leptin and single-chain follicle-stimulating hormone (scFSH) scaffolds combined using n = 1-3 to generate a heterodimeric structure with a new function.[18] Furthermore, a homo-dimeric repebody specific for human interleukin 6 was generated using the G_4S linker along with a SpyTag and SpyCatcher protein ligation system to prolong its blood half-life and enhance clearance.[4] Two αRep homo-bidomains (A3_A3) and a hetero-bidomain (A3_bGFPD) connected by a flexible linker (G_4S) shows that the binding of the first A3_A3 bidomain ligand facilitates the binding of the second bidomain.[19] However, connecting α-helical domains from DARPin-DARPin fusion proteins with different bi- and trivalent constructs requires rigid linkers to retain binding affinity and specificity.[20]

Sridhar et al.[21] previously introduced a molecular simulation to demonstrate that natural proteins can be swapped with certain inverted peptide sequences and that the artificial proteins retain their native folding. In addition, the refolding of the C-terminus of partial unfolded ankyrin repeat protein using an intact N-terminal template structure generated an ankyrin structure similar to that from the native folding pathway.

We fused two Ank1D4 domains with $(G_4S)_4$ for structural flexibility and solubility and considered the orientation of dimeric Ank1D4 in two platforms. The first platform connects the C-terminus of an Ank1D4 module to the N-terminus of another module using a flexible linker ($Ank1D4_{NC\text{-}NC}$). The second platform was constructed by inverting the amino acid sequence of the second Ank1D4 module to fuse with the C-terminus of the first module ($Ank1D4_{NC\text{-}CN}$). $Ank1D4_{NC\text{-}CN}$ had a 15-fold and 36-fold higher binding activity than $Ank1D4_{NC\text{-}NC}$ and Ank1D4 monomer, respectively. Homo-dimeric $Ank1D4_{NC\text{-}CN}$ may be a candidate for enhancing the protection efficiency of HIV gene therapy.

Materials and methods

Design and construction of recombinant dimeric $Ank1D4_{NC\text{-}NC}$ and $Ank1D4_{NC\text{-}CN}$

The 6×His dimeric $Ank1D4_{NC\text{-}NC}$ and 6×His dimeric $Ank1D4_{NC\text{-}CN}$ gene were incorporated into plasmid pQE-30 (Qiagen, Hilden, Germany) under the control of the T5 promoter and transformed into *Escherichia coli* strain XL1-blue (Stratagene, San Diego, CA, USA) for plasmid propagation. Positive transformants harboring pQE-30-6×Hisdimeric $Ank1D4_{NC\text{-}NC}$ plasmid were confirmed using colony PCR for pQE-30-6×His dimeric $Ank1D4_{NC\text{-}NC}$ using the following primer pairs: Fw_NAnk1 (5′-TCC GCG GCC GCA GAC CTG GGT AAG-3′) and Rev_Ank23C (5′-GCT AAT TAA GCT TTG CAG GAT TTC AGC-3′). *E. coli* XL1-blue harboring plasmid pQE-30-6×His dimeric $Ank1D4_{NC\text{-}CN}$ was confirmed using these primer pairs: Fw_NAnk1 (5′-TCC GCG GCC GCA GAC CTG GGT AAG-3′)

and Rev_BstXI_Ank1D4di (5′-GAG AGA CCA TGG TTG TGG TGT CCA GAC CCT TTT TCA GCA GTT CA-3′). Plasmid DNA was purified by QuickGene Plasmid kit S II (Kurabo), sequenced (Agentide Inc, USA) and error-free clones were selected for all experiments.

Production of recombinant monomeric and dimeric Ank1D4 and capsid protein (H_6-CAp24)

pQE-30 plasmid harboring monomeric Ank1D4 and dimeric $Ank1D4_{NC-NC}$ or $Ank1D4_{NC-CN}$ were transformed into *E. coli* strain M15 (pREP4) (Qiagen, Germany) and protein expression was induced with the addition of isopropyl β-D-1-thiogalactopyranoside (IPTG) as previously described.[7] *E. coli* BL21 (DE3) encoding plasmid pTriEx-H_6CAp24 (Novagen) was used to produce recombinant H_6-CAp24.

All bacteria were cultured in 500 mL Super broth: 3% w/v tryptone, 2% w/v yeast extract, 1% w/v MOPS buffer pH 6.5-7.9, 100 µg/mL ampicillin and 25 µg/mL kanamycin containing 1% w/v glucose for Ank1D4 monomer and CAp24 and 0.05% w/v glucose for Ank1D4 dimers. The cultures were incubated at 37°C with shaking until the optical density at 600 nm (OD600) reached 0.8. Protein expression was induced by the addition of 0.1 mM IPTG for Ank1D4 monomer and $Ank1D4_{NC-NC}$ and 0.05 mM for $Ank1D4_{NC-CN}$ and cultured for 16 h at 30°C for the monomer, $Ank1D4_{NC-NC}$ and CAp24, and at 20°C for $Ank1D4_{NC-CN}$. The bacteria were collected by centrifugation at 1,400×g for 15 min at 4°C (Eppendorf AG, Germany) and washed twice with phosphate buffered saline (PBS pH 7.4). The final pellet was resuspended in PBS, subjected to the freeze-thaw technique, followed by ultrasonic processor UP100H (Hielscher, Germany) and centrifugation at 5,600×g for 30 min at 4°C.

Purification and quantification of monomeric Ank1D4 and dimeric Ank1D4

Soluble protein lysates were filtered and purified by immobilized metal ion affinity chromatography using a HisTrap™ HP column (GE Healthcare, Piscataway, NJ, USA) containing precharged Ni Sepharose™ with a ÄKTA™ pure chromatography system (GE Healthcare). The elution buffer was exchanged with PBS using Amicon® Ultra-15 centrifugal filter units (Merck KGaA, Darmstadt, Germany). The purity of the recombinant proteins was assessed by 15% sodium dodecyl sulfate polyacrylamide gel electrophoresis (SDS-PAGE) and visualized using modified Coomassie blue staining and immunoblotting. The nitrocellulose membranes were incubated with blocking solution (2% skim milk in PBS) for 16 h at 4°C. Proteins were bound by incubating with monoclonal anti-His-tag antibody (Thermo Fisher Scientific) diluted 1:3,000 in blocking solution for 2 h at room temperature (RT). After washing with PBST (PBS containing 0.05% Tween 20), membranes were incubated for 1 h at RT with goat anti-mouse Igs conjugated HRP (1:3,000 dilution in blocking solution) (KPL). After washing with PBST, the recombinant proteins were detected using 3, 3′, 5, 5′-tetramethylbenzidine (TMB) membrane peroxidase substrate (KPL) and analyzed using a ChemiDoc™ MP Imaging System (Bio-Rad). Monomeric Ank1D4, dimeric Ank1D4 and CAp24 concentrations were quantified using the Pierce™ BCA protein assay kit (Thermo Fisher Scientific, Waltham, MA, USA).

Monomeric and dimeric Ank1D4 binding properties with CAp24 protein

A capture enzyme-linked immunosorbent assay (ELISA) was used to analyze the binding of monomeric Ank1D4 or dimeric Ank1D4 with the H_6-CAp24 capture protein. A molar equivalent of immobilized dimeric (2 µg/mL) or monomeric Ank1D4 (1 µg/mL) was loaded onto the 96-well plate, washed with PBST, and incubated with 2% w/v skim milk in 1 × PBS for 1 h at RT. CAp24 in PBS with 2% w/v BSA was applied to the wells with immobilized ankyrins or control (PBS) and incubated for 1 h at RT. In house mouse anti-p24 monoclonal antibody (G18) (1 µg/mL in PBS with 2% w/v BSA) was added and incubated for 1 h at RT. After washing with PBST, a 1:3,000 dilution of goat anti-mouse immunoglobulins conjugated HRP in PBS with 2% w/v BSA was added and incubated for 1 h at RT. Ankyrin binding properties were detected by monitoring the absorbance at 450 nm in an ELISA plate reader after adding TMB substrate.

Characterization of monomeric and dimeric Ank1D4 binding sites by sandwich ELISA

Mouse anti-p17 monoclonal antibody (G53) was immobilized on the surface of a microtiter plate (Greiner) at 1 µg/mL final concentration and incubated at 4°C overnight. Plates were washed with PBST and incubated with PBS in 2% w/v BSA for 1 h at RT. Each protein was dissolved in PBS with 2% w/v BSA. Recombinant his$_6$-matrix-capsid (H_6-p17p24) was prepared from SF9 cells as previously described[7] using pBlueBac4.5 transfer vector (Invitrogen) with the Bac-N-Blue™ system (Invitrogen). H_6-p17p24 (5 µg/mL) was added to each well. Monomeric Ank1D4 (1 µg/mL), dimeric $Ank1D4_{NC-NC}$, and $Ank1D4_{NC-CN}$ were added at 2 µg/mL and incubated for 1 h at RT. Biotinylated-CAp24 2 µg/mL was added and incubated for 1 h at RT. After washing with PBST, a 1:5,000 dilution of HRP-conjugated streptavidin (KPL) was added and incubated for 1 h at RT. Binding characteristics were detected by monitoring absorbance at 450 nm after adding TMB substrate.

Binding kinetic analysis

Biolayer interferometry (BLI) was performed to analyze the binding activity of dimeric Ank1D4 compared with monomeric Ank1D4 interacting with biotinylated H_6-CAp24 using the BLItz™ system (FortéBio, Menlo Park, CA). Briefly, a streptavidin biosensor was used with immobilized biotinylated CAp24 (loading) on the surface as previously described.[14] The biotinylated CAp24-loaded biosensor was dipped into a solution containing ankyrins (association step), followed by dipping in 2% BSA in PBST (dissociation step). The binding association (k_{on}) and dissociation rate constants (k_{off}) and the equilibrium dissociation constant (K_D) were calculated by locally fitting the binding and dissociation curves using mathematical equations (k_{off}/k_{on}) in the BLItz Pro 1.1 software. The measurements were plotted using a sensorgram in real-time.

Results

Construction of dimeric Ank1D4

Two Ank1D4 monomers were connected by a flexible linker $(G_4S)_4$ to create Ank1D4$_{NC\text{-}NC}$ (**Figure 1A**) and Ank1D4$_{NC\text{-}CN}$ (**Figure 1B**). These dimers were cloned into pQE-30 plasmid containing a N-terminal histidine-6 tag and expressed in *Escherichia coli* M15 (pREP4). Protein purity was verified by SDS-PAGE (**Figure 2**) and their identity confirmed by immunoblotting using a monoclonal anti-His-tag antibody. Purified proteins were found at the expected molecular masses for monomeric (17 kDa), dimeric Ank1D4$_{NC\text{-}NC}$ (37 kDa), and Ank1D4$_{NC\text{-}CN}$ (38 kDa).

Monomeric Ank1D4 and dimeric Ank1D4 binding properties

A comparison of the binding properties between monomeric Ank1D4 and dimeric Ank1D4 interacting with CAp24 was determined using capture ELISA. Ank1D4$_{NC\text{-}NC}$ and Ank1D4$_{NC\text{-}CN}$ (2 μg/mL) showed higher absorbance in comparison with the monomer (1 μg/mL) (**Figure 3**). In addition, Ank1D4$_{NC\text{-}CN}$ captured more CAp24 molecules than Ank1D4$_{NC\text{-}NC}$. The results suggest distinct CAp24 binding behaviors of monomeric Ank1D4, Ank1D4$_{NC\text{-}NC}$, and Ank1D4$_{NC\text{-}CN}$.

Bifunctional module relies on dimeric Ank1D4 interaction with CAp24

Sandwich ELISA was used to examine whether dimeric Ank1D4 interacts with CAp24 at both binding sites compared with monomeric Ank1D4. Anti-p17 mAb (G53) was absorbed on the ELISA well, followed by H_6-p17p24 to allow interaction with the first homodimeric module. The second module binds to biotinylated CAp24 and is detected by horseradish peroxidase (HRP)-conjugated streptavidin. Monomeric Ank1D4 and Ank1D4$_{NC\text{-}NC}$ showed similar negative results indicating that each protein has one binding site (**Figure 4**). Meanwhile, Ank1D4$_{NC\text{-}CN}$ exhibited a high binding signal showing that this dimer has dual CAp24 binding sites and the binding of the first module has a positive effect on the second.

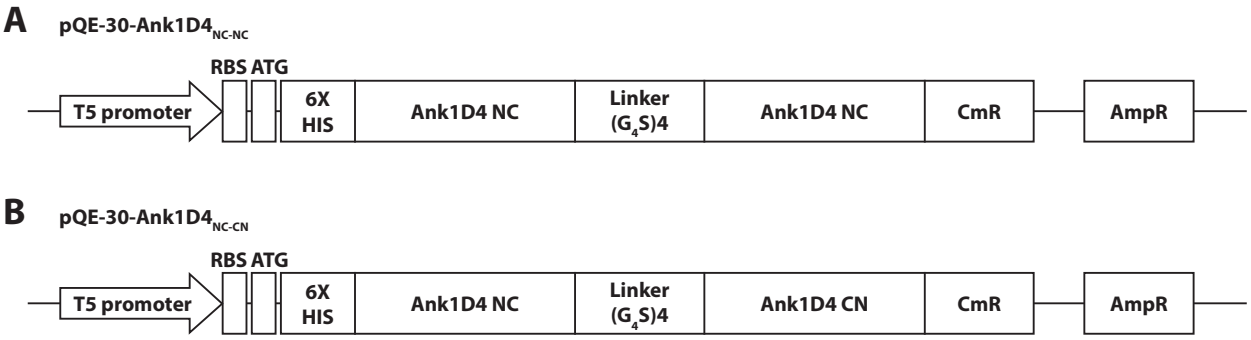

Figure 1. Construction of pQE-30 plasmid encoding dimeric Ank1D4$_{NC\text{-}NC}$ (A) and dimeric Ank1D4$_{NC\text{-}CN}$ (B) with $(G_4S)_4$ linkers. These plasmids were expressed with a hexa-histidine tag upstream of ankyrin modules and controlled by the T5 promoter. CmR and AmpR refer to chloramphenicol and ampicillin resistance cassettes, respectively, RBS is the ribosome binding site (AGGAGA), while ATG is the start codon.

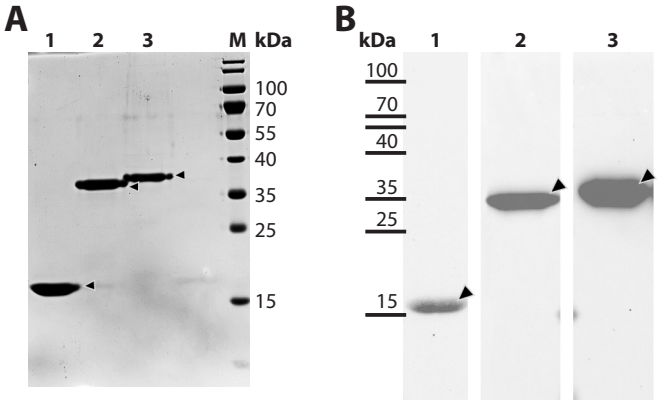

Figure 2. Expression and purification of recombinant monomeric and dimeric Ank1D4. (A) Analysis of his-tag purified recombinant monomeric Ank1D4 (Lane 1), dimeric Ank1D4$_{NC\text{-}NC}$ (Lane 2), and Ank1D4$_{NC\text{-}CN}$ (Lane 3) by SDS-PAGE. (B) Immunoblotting of ankyrins with monoclonal anti-His-tag antibody. M, protein molecular weight markers and arrow, bands of interest. Apparent molecular masses of monomeric Ank1D4, dimeric Ank1D4$_{NC\text{-}NC}$, and Ank1D4$_{NC\text{-}CN}$ are 17, 37 and 38 kDa, respectively.

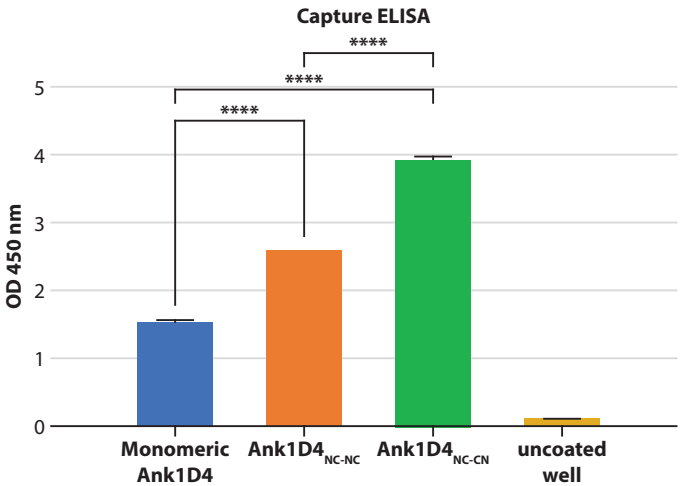

Figure 3. Capture ELISA determination of ankyrin binding to CAp24. Molar equivalent immobilization of monomeric and dimeric Ank1D4 on a 96-well plate, incubation with CAp24, anti-CAp24 mAb (G18), and detection with HRP-conjugated goat anti-mouse immunoglobulin. Absorbance at 450 nm was measured after adding TMB substrate. The data are stated as the mean ± SD from three independent experiments. ****P < 0.0001 using one-way ANOVA.

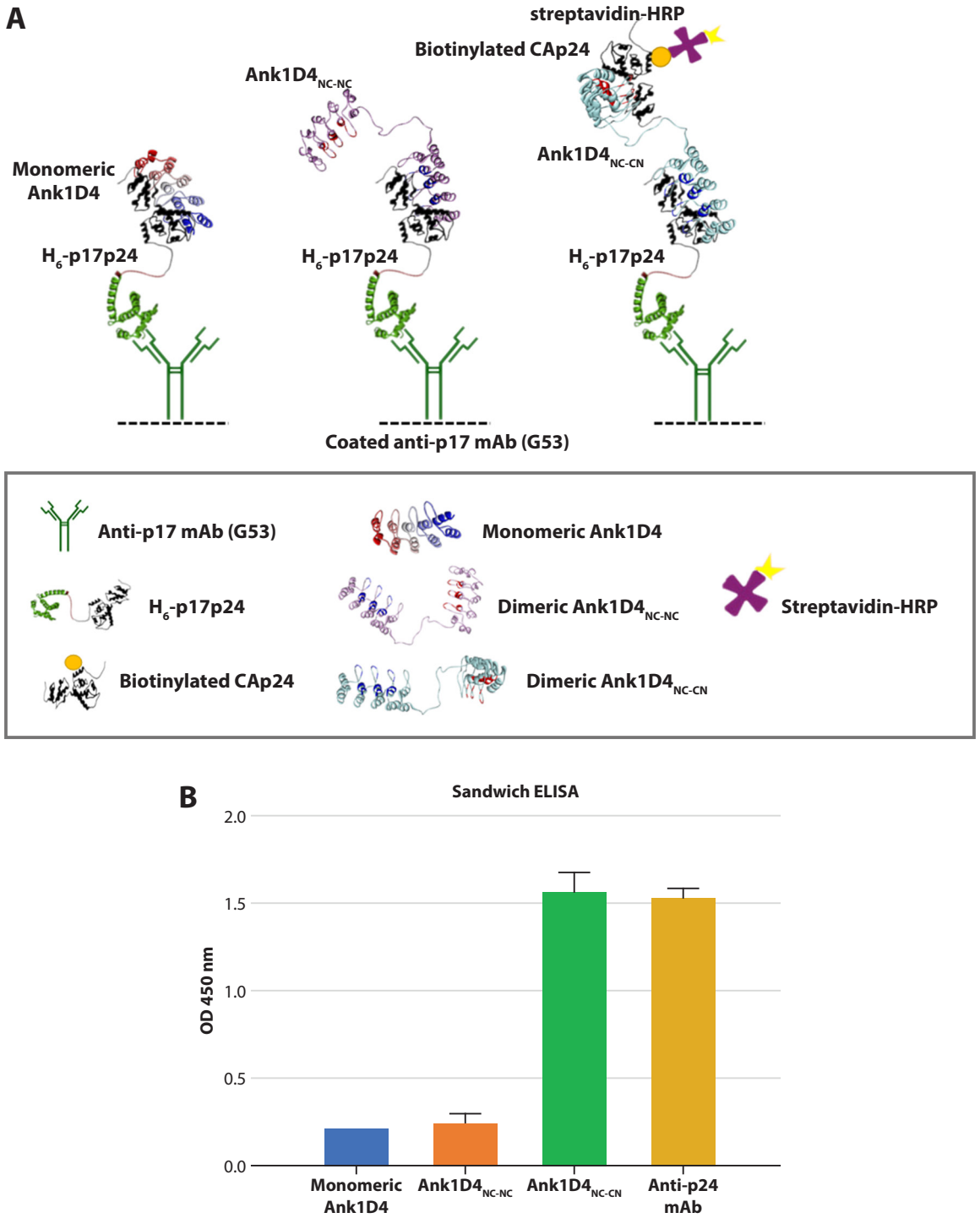

Figure 4. Binding characteristics of monomeric and dimeric Ank1D4 detected by sandwich ELISA. (A) Schematic diagram of sandwich ELISA. (B) Anti-p17 mAb (G53) was immobilized in a 96-well plate to capture H_6-p17p24 followed by the addition of Ank1D4 monomer or Ank1D4 dimers, then biotinylated CAp24. Ankyrin-bound biotinylated CAp24 was detected using HRP-conjugated streptavidin by measuring the absorbance at 450 nm after adding TMB substrate. Anti-p24 mAb (G18) is specific to CAp24. It is used to demonstrate the bifunctional property in this system for interpreting the binding property of monomeric and dimeric Ank1D4.

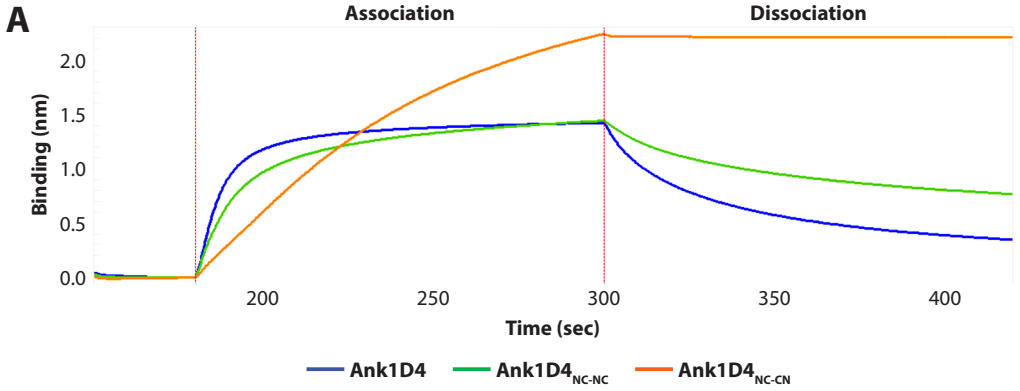

B

Variants	k_{on} (1/Ms)	k_{off} (1/s)	K_D (nM)
Monomeric Ank1D4	2.1×10^5	2.7×10^{-2}	126.2 ± 3.6
Dimeric Ank1D4$_{NC-NC}$	1.9×10^5	1.0×10^{-2}	53.7 ± 5.0
Dimeric Ank1D4$_{NC-CN}$	5.8×10^4	1.5×10^{-4}	3.5 ± 2.9

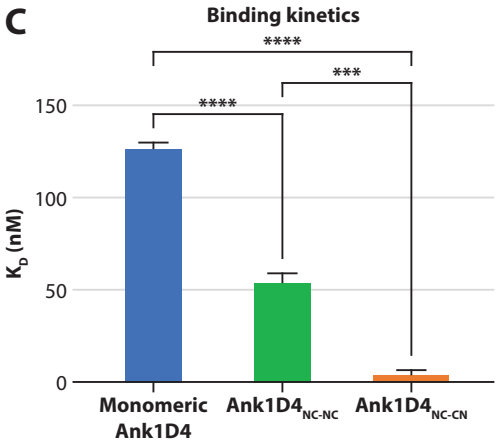

Figure 5. Comparison of dimeric Ank1D4 and monomeric Ank1D4 binding kinetics with CAp24. The streptavidin biosensor is immobilized with biotinylated CAp24 and monomeric or dimeric Ank1D4 is added at 10 μg/mL. (A) Sensorgram of binding kinetic of the association and dissociation for Ank1D4, Ank1D4$_{NC-NC}$, and Ank1D4$_{NC-CN}$ towards biotinylated CAp24. (B) Kinetic rate constants (k_{on} and k_{off}) and (C) comparison of the equilibrium dissociation constant of monomeric Ank1D4, Ank1D4$_{NC-NC}$, and Ank1D4$_{NC-CN}$ were calculated by KD = k_{off}/k_{on}. The k_{on} rate is measured in per moles per second ($M^{-1}s^{-1}$) whereas k_{off} is measured in per seconds (s^{-1}). The BLI analysis presented as the mean ± SD from three independent experiments. ***$P < 0.001$ and ****$P < 0.0001$ were determined by one-way ANOVA. Assays were analyzed by BLItz™.

CAp24-binding kinetics of dimeric Ank1D4$_{NC-NC}$ and Ank1D4$_{NC-CN}$

The binding kinetics of monomeric Ank1D4, Ank1D4$_{NC-NC}$ and Ank1D4$_{NC-CN}$ were displayed in the sensorgram (**Figure 5A**). The equilibrium dissociation constant (KD) of Ank1D4$_{NC-NC}$ (53.7 ± 5.0 nM) and Ank1D4$_{NC-CN}$ (3.5 ± 2.9 nM) is significantly stronger than that of the monomer (126.2 ± 3.6 nM) (**Figure 5B and C**). The association rate of Ank1D4$_{NC-NC}$ is comparable to that of monomeric Ank1D4 by BLI analysis while Ank1D4$_{NC-CN}$ is the slowest. These results strongly support the sandwich ELISA data indicating that Ank1D4$_{NC-CN}$ has two binding sites, while Ank1D4$_{NC-NC}$ has only one prominent binding site with a much weaker second binding site.

Discussion

We previously reported the interference of CAp24-specific HIV-1 assembly processes by Ank1D4[7,8] at the inner membrane. Although a reduction in viral production was observed, the binding affinity of Ank1D4 for CAp24 marginally improved by mutating Ank1D4 and CAp24 using a rational design, as the interaction energies were not significantly altered.[14]

In this study, the avidity of Ank1D4 is addressed by the generation of homodimers. Generally, there are two alternative empirical linkers to generate dimers: rigid and flexible. Recently, a DARPin-DARPin dimer was designed using a rigid linker avoiding flexible linkers that begin and end with α-helices.[20] However, the drawback of rigid linkers is that relatively long structures may be required if sufficient separation of protein domains is required. The heterodimeric TcdB-neutralizing DARPins were created by joining individual monomeric DARPins via a flexible linker $(G_4S)_3$ to inhibit *Clostridium difficile* infection. However, the reverse configuration of TcdB-specific DARPin led to loss of the bispecific function.[22] A longer flexible linker $(G_4S)_4$ between DARPin monomers simultaneously recognized two distinct FcεRIα domains with the proper orientation of DARPin units.[23] In addition, the $(G_4S)_4$ linker in bivalent DARPin G3_G3 results in high avidity against HER2.[24] In this study, we analyzed if Ank1D4 dimers (Ank1D4$_{NC-NC}$, and Ank1D4$_{NC-CN}$) with a flexible linker $(G_4S)_4$ have increased avidity for CAp24 and tested for the occurrence of dual binding sites.[25] Both dimeric forms bind CAp24 with higher affinity than the monomeric form by capture ELISA

although Ank1D4$_{NC-CN}$ has a significantly higher binding signal than Ank1D4$_{NC-NC}$. Sandwich ELISA strongly suggests that dimeric Ank1D4$_{NC-CN}$ has a bifunctional module and captures two CAp24 molecules per dimer while Ank1D4$_{NC-NC}$ dimer and Ank1D4 monomer has only one CAp24 binding site. These results suggest that there are conformational differences between the binding surfaces of the two dimeric ankyrins.

Structural analysis of the dimers was performed to clarify the CAp24 binding discrepancy. Comparison of the inverted second module of Ank1D4$_{NC-CN}$ with that of the original Ank1D4 shows that Ank1D4$_{NC-CN}$ forms ankyrin dimers upon validation of active amino acids residing in the Ank1D4 helix loop. Several *in silico* studies support the idea that certain inverted peptide sequences fold with a natural conformation.[21,26] The structure of retro-protein A forming a three-helix bundle was conserved and stabilized using a lattice model.[26] Pal-Bhowmick et al. formerly reported the misfolding of retro S peptide, however, it was synthesized *in vitro*.[27] Meanwhile, ankyrin dimers were produced in *E. coli* containing chaperones GrpE, DnaK and DnaJ to support the proper folding mechanism of the protein.[28] The kinetics of reversible *in vitro* refolding of unfolded ankyrin suggest that it relies on the specific protein type.[29] The rapid folding kinetics of ankyrin probably advocates this phenomenon. The novel inverted ankyrin (Ank1D4$_{NC-CN}$) in this study retains functional binding activity. Therefore, the parent-like structure of inverted Ank1D4 is beneficial for determining the avidity of Ank1D4$_{NC-CN}$.

The association rate among three ankyrin forms suggested that there is a greater folding energy barrier of intermediates in Ank1D4$_{NC-CN}$, with the initial formation of unstructured subunits followed by folding into bifunctional subunits.[30] This indicates that Ank1D4$_{NC-NC}$ and Ank1D4$_{NC-CN}$ have different conformational structures. Ank1D4$_{NC-CN}$ demonstrates simultaneous binding with CAp24 with its K_D (3.5 ± 2.9 nM) 36-fold lower than monomeric Ank1D4 and 15-fold lower than Ank1D4$_{NC-NC}$ (53.7 ± 5.0 nM). According to the capture ELISA assay, the binding activity of Ank1D4$_{NC-NC}$ is significantly lower than Ank1D4$_{NC-CN}$. This evidence reflects superior possibly of active dimeric form in Ank1D4$_{NC-CN}$ in contrast to Ank1D4$_{NC-NC}$. In addition, the distribution of biotinylated CAp24 absorbed on the streptavidin tip in BLI is better suited for the active site distances in Ank1D4$_{NC-CN}$. The proper distance between the two targets determining the binding properties was considered.[31] If the spacing of the target is more or less than the distance between the binding surfaces, there will not be avidity improvements.

Although the improvement of biological function of ankyrin dimers has been demonstrated, the X-ray crystallography should be applied to elucidate the structures of ankyrin dimers. The conformational structures will be an additive to explain the different dimension of Ank1D4$_{NC-NC}$ and Ank1D4$_{NC-CN}$, which reflects the distinct binding activity.

Potential conflicts of interest

The authors declare no conflicts of interest in relation to this study.

Acknowledgements

This work was supported by the Distinguished Research Professor Grant (NRCT 808/2563) of the National Research Council of Thailand, the Office of National Higher Education Science Research and Innovation Policy Council, the Program Management Unit for Human Resources & Institutional Development, Research and Innovation [B05F630102], The National Science and Technology Development Agency (NSTDA) and The National Research University project under Thailand's Office of the Higher Education Commission.

References

1. Škrlec K, Štrukelj B, Berlec A. Non-immunoglobulin scaffolds: a focus on their targets. Trends Biotechnol. 2015;33(7):408-18.
2. Hadpech S, Nangola S, Chupradit K, Fanhchaksai K, Furnon W, Urvoas A, et al. Alpha-helicoidal HEAT-like Repeat Proteins (αRep) Selected as Interactors of HIV-1 Nucleocapsid Negatively Interfere with Viral Genome Packaging and Virus Maturation. Sci Rep. 2017;7(1):1-19.
3. Forrer P, Stumpp MT, Binz HK, Plückthun A. A novel strategy to design binding molecules harnessing the modular nature of repeat proteins. FEBS Lett. 2003;539(1-3):2-6.
4. Kim TY, Seo HD, Lee J jae, Kang JA, Kim WS, Kim HM, et al. A dimeric form of a small-sized protein binder exhibits enhanced anti-tumor activity through prolonged blood circulation. J Control Release. 2018;279:282-91.
5. Vazquez-Lombardi R, Phan TG, Zimmermann C, Lowe D, Jermutus L, Christ D. Challenges and opportunities for non-antibody scaffold drugs. Drug Discov Today. 2015;20(10):1271-83.
6. Schweizer A, Rusert P, Berlinger L, Ruprecht CR, Mann A, Corthésy S, et al. CD4-specific designed ankyrin repeat proteins are novel potent HIV entry inhibitors with unique characteristics. PLoS Pathog. 2008;4(7): 14-8.
7. Nangola S, Urvoas A, Valerio-Lepiniec M, Khamaikawin W, Sakkhachornphop S, Hong SS, et al. Antiviral activity of recombinant ankyrin targeted to the capsid domain of HIV-1 Gag polyprotein. Retrovirology. 2012;9(1):17.
8. Sakkhachornphop S, Hadpech S, Wisitponchai T, Panto C, Kantamala D, Utaipat U, et al. Broad-spectrum antiviral activity of an ankyrin repeat protein on viral assembly against chimeric NL4-3 viruses carrying Gag/PR derived from circulating strains among northern thai patients. Viruses. 2018;10(11).
9. Thirunavukarasu D, Udhaya V, Iqbal HS, Umaarasu T. Patterns of HIV-1 Drug-Resistance Mutations among Patients Failing First-Line Antiretroviral Treatment in South India. J Int Assoc Provid AIDS Care. 2016;15(3):261-8.
10. Avi R, Pauskar M, Karki T, Kallas E, Jogeda EL, Margus T, et al. Prevalence of drug resistance mutations in HAART patients infected with HIV-1 CRF06_cpx in Estonia. J Med Virol. 2016;88(3):448-54.
11. Cannon P, June C. Chemokine receptor 5 knockout strategies. Curr Opin HIV AIDS. 2011;6(1):74-9.
12. Mohammadzadeh S, Rajabibazl M, Fourozandeh M, Rasaee MJ, Rahbarizadeh F, Mohammadi M. Production of recombinant scFv against p24 of human immunodeficiency virus type 1 by phage display technology. Monoclon Antibodies Immunodiagn Immunother. 2014;33(1):28-33.
13. Che Omar MT. Expression of Functional Anti-p24 scFv 183-H12-5C in HEK293T and Jurkat T Cells. Adv Pharm Bull. 2017;7(2):299-312.
14. Saoin S, Wisitponchai T, Intachai K, Chupradit K, Moonmuang S, Nangola S, et al. Deciphering critical amino acid residues to modify and enhance the binding affinity of ankyrin scaffold specific to capsid protein of human immunodeficiency virus type 1. Asian Pac J Allergy Immunol. 2018;36(2):126-35.

15. Sornsuwan K, Thongkhum W, Pamonsupornwichit T, Carraway TS, Soponpong S, Sakkhachornphop S, et al. Performance of affinity-improved darpin targeting HIV capsid domain in interference of viral progeny production. Biomolecules. 2021;11(10):1-17.
16. Xue F, Gu Z, Feng JA. LINKER: A web server to generate peptide sequences with extended conformation. Nucleic Acids Res. 2004;32: 562-5.
17. Liu C, Chin JX, Lee DY. SynLinker: An integrated system for designing linkers and synthetic fusion proteins. Bioinformatics. 2015;31(22):3700-2.
18. Peng Y, Zeng W, Ye H, Han KH, Dharmarajan V, Novick S, et al. A General Method for Insertion of Functional Proteins within Proteins via Combinatorial Selection of Permissive Junctions. Chem Biol. 2015;22(8):1134-43.
19. Léger C, Di Meo T, Aumont-Nicaise M, Velours C, Durand D, Li de la Sierra-Gallay I, et al. Ligand-induced conformational switch in an artificial bidomain protein scaffold. Sci Rep. 2019;9(1):1-13.
20. Wu Y, Batyuk A, Honegger A, Brandl F, Mittl PRE, Plückthun A. Rigidly connected multispecific artificial binders with adjustable geometries. Sci Rep. 2017;7(1):11217.
21. Sridhar S, Guruprasad K. Can Natural Proteins Designed with 'Inverted' Peptide Sequences Adopt Native-Like Protein Folds? PLoS One. 2014; 9(9):e107647.
22. Simeon R, Jiang M, Chamoun-Emanuelli AM, Yu H, Zhang Y, Meng R, et al. Selection and characterization of ultrahigh potency designed ankyrin repeat protein inhibitors of C. Difficile toxin B. PLoS Biol. 2019;17(10): 1-32.
23. Eggel A, Baumann MJ, Amstutz P, Stadler BM, Vogel M. DARPins as Bispecific Receptor Antagonists Analyzed for Immunoglobulin E Receptor Blockage. J Mol Biol. 2009;393(3):598-607.
24. Theurillat JP, Dreier B, Nagy-Davidescu G, Seifert B, Behnke S, Zürrer-Härdi U, et al. Designed ankyrin repeat proteins: A novel tool for testing epidermal growth factor receptor 2 expression in breast cancer. Mod Pathol. 2010;23(9):1289-97.
25. Zahnd C, Kawe M, Stumpp MT, De Pasquale C, Tamaskovic R, Nagy-Davidescu G, et al. Efficient tumor targeting with high-affinity designed ankyrin repeat proteins: Effects of affinity and molecular size. Cancer Res. 2010;70(4):1595-605.
26. Olszewski KA, Kolinski A, Skolnick J. Does a backwardly read protein sequence have a unique native state? Protein Eng Des Sel. 1996;9(1):5-14.
27. Pal-Bhowmick I, Pati Pandey R, Jarori GK, Kar S, Sahal D. Structural and functional studies on Ribonuclease S, retro S and retro-inverso S peptides. Biochem Biophys Res Commun. 2007;364(3):608-13.
28. Kolaj O, Spada S, Robin S, Gerard JG. Use of folding modulators to improve heterologous protein production in Escherichia coli. Microb. 2009;8:1-17.
29. Lee W, Zeng X, Rotolo K, Yang M, Schofield CJ, Bennett V, et al. Mechanical anisotropy of ankyrin repeats. Biophys J. 2012;102(5):1118-26.
30. Shammas SL, Rogers JM, Hill SA, Clarke J. Slow, reversible, coupled folding and binding of the spectrin tetramerization domain. Biophys J. 2012;103(10):2203-14.
31. Kuil J, Van Wandelen LTM, De Mol NJ, Liskamp RMJ. Switching between low and high affinity for the Syk tandem SH2 domain by irradiation of azobenzene containing ITAM peptidomimetics. J Pept Sci. 2009;15(10): 685-91.